HAL
open science

Magnon bound states versus anyonic Majorana excitations in the Kitaev honeycomb magnet α-RuCl_3

Dirk Wulferding, Youngsu Choi, Seung-Hwan Do, Chan Hyeon Lee, Peter Lemmens, Clément Faugeras, Yann Gallais, Kwang-Yong Choi

To cite this version:

Dirk Wulferding, Youngsu Choi, Seung-Hwan Do, Chan Hyeon Lee, Peter Lemmens, et al.. Magnon bound states versus anyonic Majorana excitations in the Kitaev honeycomb magnet α-RuCl_3. Nature Communications, 2020, 11 (1), pp.1603. 10.1038/s41467-020-15370-1 . hal-03026197

HAL Id: hal-03026197

https://hal.science/hal-03026197v1

Submitted on 26 Nov 2020

HAL is a multi-disciplinary open access archive for the deposit and dissemination of scientific research documents, whether they are published or not. The documents may come from teaching and research institutions in France or abroad, or from public or private research centers.

L'archive ouverte pluridisciplinaire **HAL**, est destinée au dépôt et à la diffusion de documents scientifiques de niveau recherche, publiés ou non, émanant des établissements d'enseignement et de recherche français ou étrangers, des laboratoires publics ou privés.

Magnon bound states vs. anyonic Majorana excitations in the Kitaev honeycomb magnet α-$RuCl_3$

Dirk Wulferding,[1,2,*] Youngsu Choi,[3,†] Seung-Hwan Do,[3] Chan Hyeon Lee,[3]
Peter Lemmens,[1,2] Clément Faugeras,[4] Yann Gallais,[5] and Kwang-Yong Choi[3,‡]

[1]*Institute for Condensed Matter Physics,*
TU Braunschweig, D-38106 Braunschweig, Germany
[2]*Laboratory for Emerging Nanometrology (LENA),*
TU Braunschweig, D-38106 Braunschweig, Germany
[3]*Department of Physics, Chung-Ang University, Seoul 156-756, Republic of Korea*
[4]*Laboratoire National des Champs Magnétiques Intenses,*
CNRS-UGA-UPS-INSA-EMFL, 25 avenue des Martyrs, Grenoble, 38042, France
[5]*Laboratoire Matériaux et Phénomènes Quantiques (UMR 7162 CNRS),*
Université Paris Diderot - Paris 7, 75205 Paris cedex 13, France

(Dated: August 18, 2019)

The pure Kitaev honeycomb model harbors a quantum spin liquid in zero magnetic fields, while applying finite magnetic fields induces a topological spin liquid with non-Abelian anyonic excitations. This topological phase has been much sought after in Kitaev candidate materials, such as α-RuCl$_3$. Currently, two competing scenarios are discussed for the intermediate field phase of this compound ($B = 7 - 9$ T) based on experimental as well as theoretical results, involving (i) conventional multiparticle magnetic excitations of integer quantum number and (ii) non-trivial Majorana fermionic excitations of possibly non-Abelian nature with a fractional quantum number. To discriminate between these scenarios a detailed spectroscopic investigation of magnetic excitations over a wide field-temperature phase diagram is essential. Here we present a Raman spectroscopic study revealing magnon- and multimagnon excitations on top of a fractionalized continuum in an antiferromagnetic ($B < 7$ T) and a field-polarized phase ($B > 9$ T). These conventional excitations are contrasted by low-energy quasiparticles emerging at intermediate fields, which are closely linked to a continuum of fractionalized excitations. By tracing their temperature evolution, we find fingerprints of the formation of bound states out of Majorana fermionic excitations.

I. INTRODUCTION

The search for Majorana fermions in solid-state systems has led to the discovery of several promising candidate materials for exchange-frustrated Kitaev magnets[1–6]. One of the closest realizations of a Kitaev honeycomb lattice is α-RuCl$_3$[7,8], where the spin Hamiltonian is dominated by Kitaev interaction K. Nevertheless, non-Kitaev interactions, such as Heisenberg (J) and off-diagonal symmetric exchange terms ("Γ-term"), as well as stacking faults in α-RuCl$_3$ lead to an antiferromagnetically ordered zigzag ground state below $T_N \approx 7$ K[8]. The exact values of the Hamiltonian terms have not been pinpointed, yet a general consensus on the minimal model has emerged about a ferromagnetic $K \sim$ -6 – -16 meV, as well as $\Gamma \sim$ 1 – 7 meV, and $J \sim$ -1 – -2 meV[9,10]. This set of the magnetic parameters partly obscures the presence of Majorana fermions, but the fermionic quasiparticles are well preserved at high energies and finite temperatures[11]. Indeed, many independent and complementary ex-

perimental techniques have been used to confirm and better understand the emergence of itinerant Majorana fermions and localized gauge fluxes from the fractionalization of spin degrees of freedom[9,12,13].

A promising route in understanding Kitaev physics might be the suppression of long-range magnetic order in a magnetic field, with the possibility of generating an Ising topological quantum spin liquid at a critical field of $B_c \sim 6-7$ T[14–16]. Higher magnetic fields lead to a trivial spin polarized state. In the intermediate field range of 7-9 T, the magnetic order melts into a quantum disordered phase, in which the half-integer quantized thermal Hall conductance is observed. This remarkable finding may be taken as evidence for a field-induced topological spin liquid with chiral Majorana edge states and the central charge $q = \nu/2$ (Chern number $\nu = 1$)[13]. However, it is less clear whether such a chiral spin liquid state can be stabilized against a relatively large field and non-Kitaev terms in α-$RuCl_3$. In the original Kitaev honeycomb model, non-Abelian Majorana excitations are created upon breaking time-reversal symmetry, e.g., through applying a magnetic field[17]. These composite quasiparticles correspond to bound states of localized fluxes and itinerant Majorana fermions (see the sketch of Fig. 2a)[18]. The composite bound states are of neither fermionic nor bosonic character, but instead follow anyonic statistics that acquire an additional phase in the wavefunction upon interchanging particles[19]. For the perturbed Kitaev system bound itinerant Majorana fermions are possible, yet the stability of the topological spin liquid is poorly understood. In particular, a remaining open issue is whether the observed thermal Hall effect is a fingerprint of a non-Abelian phase featuring anyonic Majorana excitations. There exists another scenario in which the intermediate phase is smoothly connected to the fully polarized phase and the transition through B_c involves conventional multiparticle excitations due to anisotropic interactions[20]. To resolve these opposing views, one needs to clarify the nature of quasiparticle excitations emergent in the intermediate-to-high-field phase. While neutron scattering[21], THz spectroscopy[22], and electron spin resonance[23] have revealed a significant reconfiguration of the magnetic response through B_c, these methods do not suffice for obtaining a complete picture of individual quasiparticles due to limited accessible ranges of experimental parameters (energy, temperature, and field). In this work, we employ Raman spectroscopy capable of sensing magnetic excitations over the sufficiently wide ranges of temperatures $T = 2-300$ K, fields $B = 0-29$ T, and energies $\hbar\omega = 1-25$ meV ($8-200$ cm^{-1}). At low fields ($B < B_c$) and low temperatures ($T < T_N$) we observe a

number of magnetic modes superimposed onto a continuum of fractionalized excitations. Towards higher fields above 10 T, the magnetic continuum opens progressively a gap and its spectral weight is transferred to well-defined sharp excitations that correspond to magnon bound states, marking the crossover to a field-polarized phase. In the intermediate phase, a weakly bound state emerges. The bound state is formed via a spectral transfer from the fractionalized continuum through an isosbestic point around 8.75 meV, and does not smoothly connect to the magnon bound states in the high-field phase. Our results suggest that this weakly bound state carries Majorana flavor[11,24] and that the intermediate-field phase of α-$RuCl_3$ is a promising platform for testing anyonic statistics.

II. RESULTS

To elucidate the field-evolution of the magnetic excitation spectrum of α-$RuCl_3$ we performed Raman scattering experiments on oriented single crystals (see Supplementary Information I for a detailed outline of the scattering geometries). Fig. 1a showcases the representative raw spectra obtained at increasing fields aligned along the crystallographic a axis [B // (100)]. Besides two sharp, intense phonon modes at 14.5 meV and 20.5 meV [marked $E_g(1)$ and $E_g(2)$], we observe several magnetic excitations experiencing pronounced field dependence: At zero field, the magnetic Raman response consists of a broad continuum (C; green shading) and a sharp peak (M1, blue line). The latter M1 excitation at 2.5 meV is assigned to one-magnon scattering arising from a spin flip process through strong spin-orbit coupling and enables us to trace a gap of low-lying excitations at the Γ-point as a function of field. The green-shaded continuum agrees with several previous Raman scattering studies[12,25,26] and dominantly comprises Majorana fermionic excitations stemming from a fractionalization of spin degrees of freedom in the Kitaev honeycomb model[17]. Although we cannot exclude an incoherent multimagnon contribution to the continuum, the exotic temperature evolution of the continuum supports the notion of Majorana fermions[27]. As detailed in the Supplementary Information III, we find further evidence of Majorana fermionic excitations from their more prominent fermionic character at $B = 6.7$ T (when zigzag order is suppressed) compared to $B = 0$ T. As the magnetic field increases above 10 T, C becomes gapped and its spectral width narrows down. This leads to a build-up of spectral weight towards the edge of the gap (solid line in Fig. 1b-d).

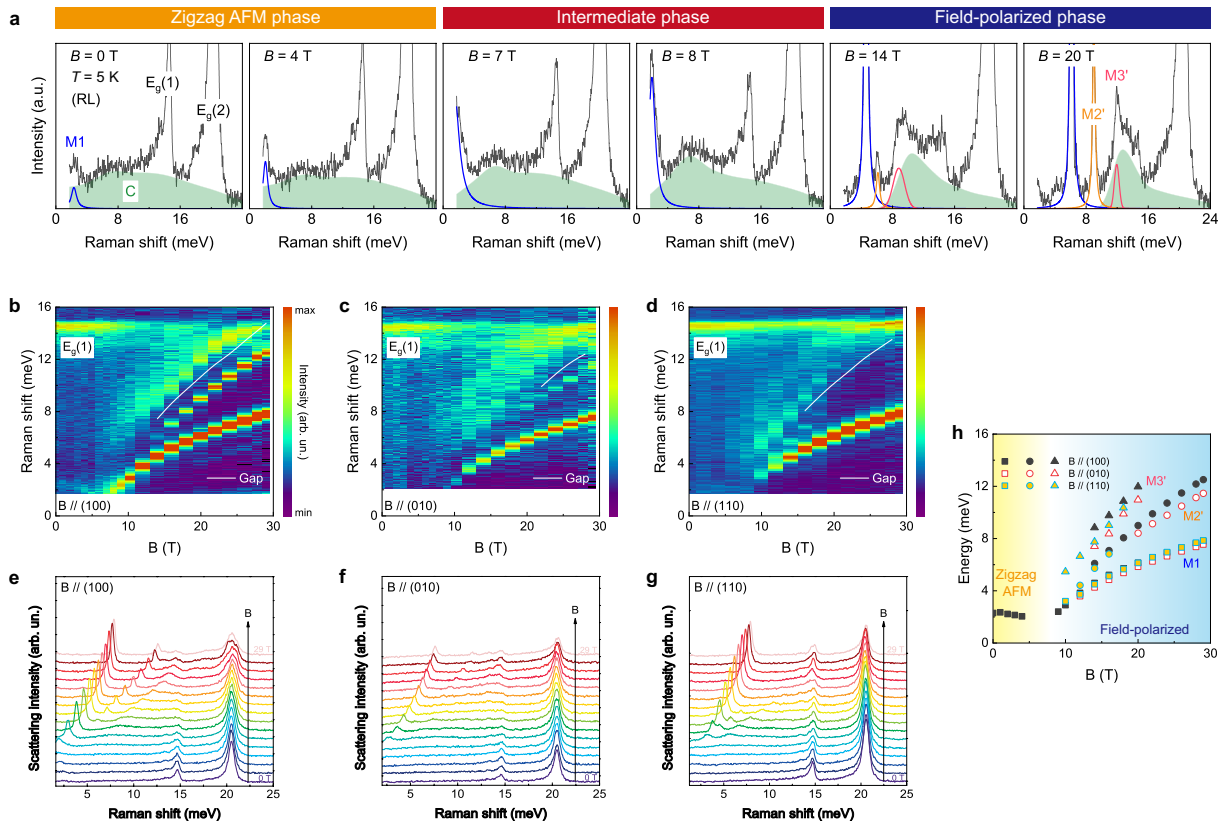

FIG. 1. **Field evolution of magnetic excitations in α-RuCl$_3$ through field-induced phases.** **a**, As-measured Raman spectra at $T \approx 5$ K. For $H//a$ α-RuCl$_3$ passes successively from a zigzag antiferromagnetic- through an intermediate- to a field-polarized-phase with increasing magnetic fields. The color shading denotes the broad continuum (C) on top of well-defined sharp peaks (M1, M2', M3') and phonon modes ($E_g(1)$ and $E_g(2)$). **b**, **c**, and **d**, Color contour plots of the Raman scattering intensity evolution with magnetic fields aligned along (100), (010), and (110), respectively. **e-g**, Their respective sets of raw Raman data. **h**, Field-dependence of the sharp low-energy magnetic excitations compared for different field directions.

Noteworthy is that the continuum has a finite intensity even at high fields $B > B_c$, while several sharp and well-defined excitations emerge additionally with increasing fields. The residual spectral weight of C at sufficiently high fields means that spin excitations are richer than the multiparticle magnons. We recall that recent numerical calculations on the field effect of the Kitaev model uncover a wide Kitaev paramagnetic region, namely, far beyond the critical field and at finite temperature[28]. In this light, we ascribe the gapped continuum excitations to fractional quasiparticles pertinent to the Kitaev paramagnetic

state. The M1 peak is ubiquitous in all measured fields. The M2' excitation (orange line) is split off from the M1 peak above 12 T, while the higher-energy M3' excitation (red line) appears inside the gapped continuum above 10-14 T. In consideration of the spectral form and energy, the M2' and M3' peaks are assigned to two and three magnon bound states, respectively. In previous experimental field-dependent studies on α-$RuCl_3$ ranging from inelastic neutron scattering (INS)[21], to THz absorption[22], to ESR[23] such well-defined magnetic excitations were reported and interpreted in terms of one-magnon or magnon bound states. Raman scattering probes a spin-conserving process ($\Delta S_z = 0$), which could unravel new aspects of low-energy excitations since the above methods are insensitive to a singlet sector. Furthermore, while first-order Raman scattering processes are restricted to $k \approx \Gamma$, higher-order scattering processes probe regions of large density of states across the Brillouin zone, which distinguishes Raman scattering from methods like THz- or ESR-spectroscopy. The evolution of all magnetic excitations as a function of fields up to 29 T is depicted in the color contour plots of Figs. 1b, 1c, and 1d together with the as-measured Raman spectra in Figs. 1e, 1f, and 1g for field directions along (100), (010), and (110), respectively. A slight anisotropy in magnetic excitations as a function of field-direction becomes apparent, which is highlighted in the plot in Fig. 1h. In particular, the energy and field ranges of M3' are sensitive to the in-field directions, indicating the presence of non-negligible in-plane anisotropic terms. Our high-field Raman data evidence the existence of multi-magnon bound states and a gapped continuum that characterizes the spin dynamics of the partially polarized phase. However, we can extract little information on the intermediate phase because the base temperature is restricted above $T = 5$ K.

In order to study the intermediate phase in detail we switched to a magneto-optical cryostat setup, enabling us to reach a base temperature of $T = 2$ K in a field range of $B = 0-10$ T. In this scattering geometry the sample is slightly tilted away from the in-plane field geometry by an angle of 18°, resulting in an additional small but finite out-of-plane field component. Note that here both magnetic field direction as well as light scattering geometry are slightly different from the high-field setup, which prohibits a strict one-to-one comparison. Nonetheless, a good correspondence is found between the high-field B//(110) data at $T \approx 5$ K and the magneto-optical data at $T = 9$ K (see Supplementary Information I). The field-induced intermediate regime in a Kitaev magnet is a promising platform for realizing a non-Abelian phase[17], which possesses chiral Majorana states at the edge and

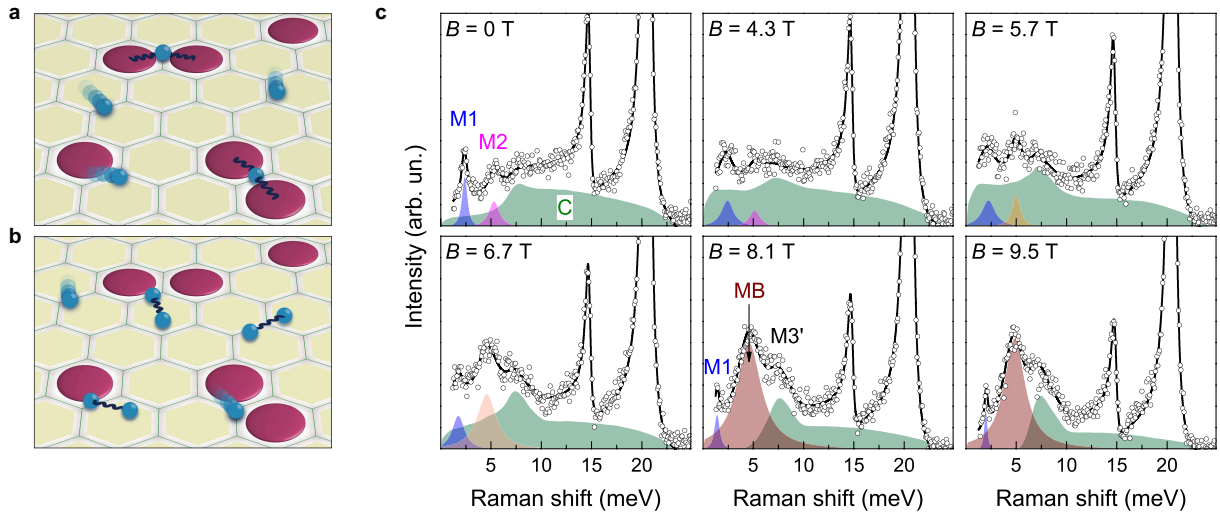

FIG. 2. **Magnetic excitations at intermediate magnetic fields.** **a**, The creation of a bound state from itinerant fermions bound to localized fluxes and **b**, from binding only itinerant Majorana fermions. **c**, Evolution of Raman data obtained at $T = 2$ K (open circles) with increasing fields from 0 T - 9.5 T. The shaded regions denote the decomposition of the magnetic excitations into well-defined peaks and a continuum of excitations. The solid line is a sum of all excitations. The M1 (blue) and M2 (purple shading) modes at low fields of 0 - 4.3 T correspond to spin wave excitations. The excitation MB (dark red) above the critical field of 6.7 T is assigned to a Majorana bound state.

anyonic excitations in the bulk. Given that the half-integer thermal Hall conductance is evidence for the chiral state, a detection of the Majorana bound states will provide its ultimate confirmation. In the extended Kitaev system, these bound states can occur in different channels[18], namely, from either binding itinerant Majorana fermions to localized fluxes (sketched in Fig. 2a), or by binding two itinerant Majorana fermions (sketched in Fig. 2b). With this in mind, we inspect the field-dependence of Raman spectra measured at $T = 2$ K, shown in Fig. 2c. Compared to the $T = 5$ K high-field data shown in Fig. 1a, the $T = 2$ K data show a new sharp structure at 5 meV (M2) in addition to the one-magnon excitation (M1) and the fractionalized continuum (C). As the field increases, the respective modes evolve in a disparate manner. Initially (at $B = 0 - 4.3$ T), the M1 and M2 modes are slightly suppressed, while the continuum C is partially renormalized towards lower energies. As B_c is approached and through 6.7 T, the spectral weight of the continuum is massively redistributed. A new low-energy mode (MB) evolves from the low-field M2 mode with a

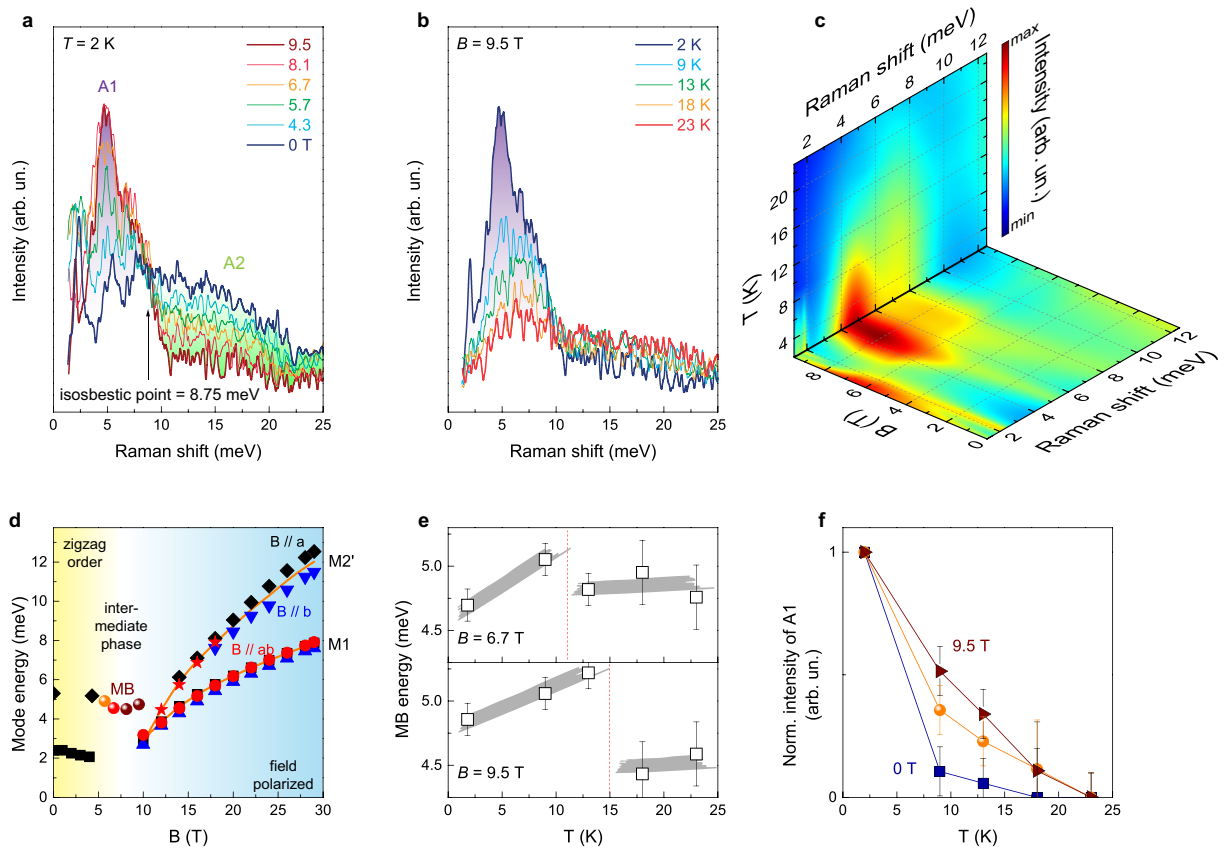

FIG. 3. **Spectral weight redistribution and formation of a bound state through B_c.** **a**, Raman spectra obtained at $T = 2$ K with increasing magnetic fields. **b**, Raman spectra at $B = 9.5$ T recorded with increasing temperatures. Phonon modes are subtracted in (a) and (b) for better visualization of the magnetic excitations. **c**, Contour plot of the magnetic Raman scattering intensity as a function of temperature and field. **d**, Field-dependence of excitations around the intermediate phase (spheres) together with spin-wave excitations at low and high magnetic fields. **e**, Thermally induced binding-unbinding crossover at $B = 6.7$ T and 9.5 T. Grey lines are guides to the eyes. **f**, Thermal melting of the low-temperature magnetic modes at 0 T, 6.7 T, and 9.5 T. Standard deviations in (e)-(f) are indicated by error bars.

shoulder structure (M3') and the continuum of Majorana excitations is gapped above 8.1 T, consistent with the data presented in Fig. 2c. A recent INS study reported a similarly broad, emerging mode in the intermediate field-induced phase[21]. It was tentatively discussed within the framework of Majorana bound states, but an ultimate assignment was hindered by the lack of a detailed temperature study.

To analyze the field-induced spectral weight redistribution carefully, we replot phonon-

subtracted Raman data taken at $T = 2$ K in Fig. 3a. With increasing field a distinct transfer of spectral weight from the mid-energy (green-shaded A2) to the low-energy regime (purple-shaded A1) is observed, with an isosbestic point located around $\omega_{\text{iso}} = 8.75$ meV, at which the magnetic Raman response is independent of the external field. The systematic field-induced redistribution of spectral weight through the isosbestic frequency suggests an intimate connection between the continuum and the newly formed excitation, and therefore supports the concept that a low-energy Majorana bound state (MB) is formed by a confinement of the high-energy broad continuum of Majorana fermionic excitations. Consistent with the high-field data presented in Fig. 1, we observe a remaining finite continuum of Majorana fermions at 9.5 T, i.e., corresponding to the non-trivial quantum spin liquid phase. A coexistence of massive Majorana fermions that form a broad, gapped continuum together with a sub-gap MB state is not compatible with the trivial polarized phase that is characterized by the multimagnon bound states. Figure 3b shows the thermal evolution obtained at $B = 9.5$ T (see Supplementary Information IV for full data set). As the temperature increases, the low-energy mode MB gradually loses in intensity and shifts towards higher energies. Meanwhile, the continuum C slightly gains in intensity. The field- and thermal evolution of magnetic modes is visualized in a contour plot in Fig. 3c, based on fits to the as-measured data. It especially highlights the similar evolution of MB with field and temperature: around 5 meV its spectral weight starts to appear at 4.7 T and grows with increasing field, while it becomes thermally stabilized upon cooling below 12 K at 9.5 T. This suggests that quantum and classical fluctuations play the same role in the confinement-deconfinement crossover due to a proximate Kitaev paramagnetic state at finite temperature[11].

Fig. 3d plots the energy of the MB mode as a function of field together with the spin-wave excitations observed in the zigzag ordered phase as well as in the high field spin-polarized phase. We note a smooth transition from M2 to MB through B_c. This weak field-dependence suggests that the MB mode corresponds to an excitation in the singlet sector ($\Delta S_z = 0$), to which Raman spectroscopy is a natural probe. As the magnon corresponds to a condensation of Majorana fermions, the M2-to-MB mode evolution may be interpreted in terms of a condensation-to-confinement crossover where the multimagnon excitations observed at low field gradually evolve into Majorana bound states. Since the continuum of deconfined Majorana excitations above B_c is massively gapped with an onset energy of 4-6 meV (see Figs. 1b-1d, Fig. 2c), the low-energy bound state can be naturally created

within the gap due to confinement. Unlike the M2-to-MB mode crossover below B_c, the MB mode is not smoothly linked to the M2' bound state for fields above B_c. Rather, as the field is lowered through 10 T, the M2' mode merges with the M1 mode, while the MB mode appears. This discontinuous evolution of quasiparticle excitations is contrasted by the rather smooth transition observed in ESR experiments through 10 T[23]. Recalling the different selection rules for quasiparticle excitations in Raman vs. ESR suggests that excitation MB is of different nature than mode 'B' probed by ESR. Although some discontinuous evolution admittedly may be expected in our data due to the slightly different experimental conditions between the high-field and the magneto-cryostat setups, the temperature difference of ≈ 3 K cannot account for a jump of 1 meV. We also recall that the vanishing thermal Hall conductance around 10 T parallels the disappearance of the MB mode[13].

Further support of the MB state interpretation comes from the temperature dependence at two different magnetic fields, 6.7 T and 9.5 T (Fig. 3e). We see a clear initial increase in the MB mode energy at both fields as the temperature rises. This is contrasted by conventional (magnon) excitations, which continuously soften with increasing temperature. For bound states, however, the thermal energy competes with the binding energy[29], until eventually an unbinding takes place. Therefore, a sudden drop in mode energy occurs at around 15 K (at $B = 9.5$ T), setting the binding energy scale to ≈ 1.3 meV (see Supplementary Information V for details). Correspondingly, in a smaller magnetic field of only 6.7 T an unbinding already occurs around $T \approx 10$ K. In contrast, the shoulder of built-up Majorana fermionic excitations gives no clear sign of binding. The thermal evolution of area A1, summarized in Fig. 3f, highlights the gradual melting of the bound state at 9.5 T (dark red triangles) with increasing temperature, while the conventional magnetic excitations at 0 T (blue squares) abruptly vanish above T_N. All these observations are consistent with the picture of a quasi-bound state of Majorana fermions that is pulled below the gapped fractionalized continuum by residual interactions of non-Kitaev origin[30].

III. DISCUSSION

In the unperturbed Kitaev model, Majorana bound states involve flux pairs combined with matter Majorana fermions in a $\Delta S_z = \pm 1$ channel[17]. However, as flux excitations are largely invisible to the Raman scattering process[31], the bound states between the flux and

matter Majorana fermions barely contribute to the magnetic Raman signal. In the presence of perturbed terms, the bound state between matter Majorana fermions is proliferated (see the cartoon in Fig. 2b)[18]. As Raman scattering probes the $\Delta S_z = 0$ channel, we conclude that the MB mode largely consists of the matter Majorana bound states. This interpretation is supported by the smooth crossover from the multi-magnon M2 mode to the bound state MB through B_c (see Figure 3d). In such a case, α-$RuCl_3$ as an apt realization of the $K-\Gamma$ model (see Supplementary Information IV) can host an exotic intermediate-field phase. In relation to this issue, we mention that a numerical study of the $J-K-\Gamma-\Gamma'$ model shows an extended regime of a chiral spin liquid for the out-of-plane field. As the magnetic field is tilted significantly towards the in-plane direction, the intermediate topological phase vanishes[32]. This discrepancy raises the challenging question whether the recently reported field-induced phase has a non-Abelian nature and how the in-plane intermediate phase transits to the alleged chiral spin-liquid phase, if the intermediate phase is of topologically trivial nature.

Our finding demonstrates that a non-trivial crossover from the zigzag through the intermediate to the high-field phase involves a confinement and binding of the Majorana fermions, calling for future work on how the observed matter Majorana bound states in an in-plane intermediate field phase of α-$RuCl_3$ and the non-Abelian phase predicted for out-of-field directions are related.

ACKNOWLEDGMENTS

We acknowledge the support of LNCMI-CNRS, a member of the European Magnetic Field Laboratory (EMFL), as well as important discussions with Natalia Perkins. This work was supported by "Niedersächsisches Vorab" through the "Quantum- and Nano-Metrology (QUANOMET)" initiative within the project NL-4, DFG-Le967-16, and the Excellence Cluster DFG-EXC 2123 Quantum Frontiers. The work at CAU was supported by the National Research Foundation (NRF) of Korea (Grant No. 2017R1A2B3012642).

IV. EXPERIMENTAL DETAILS

High magnetic fields up to 29 T were generated using the resistive magnet M10 at the LNCMI Grenoble. The sample was kept at a temperature $T \approx 5-10$ K and illuminated

with a 515 nm solid state laser (ALS Azur Light Systems) at a laser power $P = 0.4$ mW and a spot size of 5 μm diameter. Resulting Raman spectra were collected in Voigt geometry for in-plane fields, and in Faraday geometry for out-of-plane geometry, using a Princeton Instruments TriVista spectrometer equipped with a liquid N_2 cooled Pylon CCD.

Temperature-dependent Raman scattering experiments in intermediate fields of $B = 0 - 9.5$ T were carried out in 90° scattering geometry using a Horiba T64000 triple spectrometer equipped with a Dilor Spectrum One CCD and a Nd:YAG laser emitting at $\lambda = 532$ nm (Torus, Laser Quantum). A $\lambda/4$-plate was used to generate left- and right-circularly polarized light. The laser power was kept to $P = 4$ mW with a spot diameter of about 100 μm to minimize heating effects. A base temperature of $T_{\text{base}} = 2$ K was achieved by fully immersing the sample in superfluid He. Measurements at elevated temperatures were carried out in He gas atmosphere. From a comparison between Stokes- and anti-Stokes scattering we estimate the laser heating to be of 3 K outside the superfluid He environment. The sample temperatures are corrected accordingly. In-plane magnetic fields were applied via an Oxford Spectromag split coil system ($T = 1.5$ K – 300 K, $B_{\text{max}} = 10$ T).

---

* Contributed equally to this work.; Corresponding author: dirk.wulferding@tu-bs.de

† Contributed equally to this work.

‡ Corresponding author: kchoi@cau.ac.kr

[1] G. Jackeli, G. Khaliullin, Mott Insulators in the Strong Spin-Orbit Coupling Limit: From Heisenberg to a Quantum Compass and Kitaev Models. *Phys. Rev. Lett.* **102**, 017205 (2009).

[2] Y. Singh, *et al.*, Relevance of the Heisenberg-Kitaev Model for the Honeycomb Lattice Iridates A_2IrO_3. *Phys. Rev. Lett.* **108**, 127203 (2012).

[3] K. A. Modic, *et al.*, Realization of a three-dimensional spin-anisotropic harmonic honeycomb iridate. *Nat. Commun.* **5**, 4203 (2014).

[4] S. H. Chun, *et al.*, Direct evidence for dominant bond-directional interactions in a honeycomb lattice iridate Na_2IrO_3. *Nat. Phys.* **11**, 462-466 (2015).

[5] M. Abramchuk, *et al.*, Cu_2IrO_3: A New Magnetically Frustrated Honeycomb Iridate. *J. Am. Chem. Soc.* **139**, 15371-15376 (2017).

[6] K. Kitagawa, *et al.*, A spin-orbital-entangled quantum liquid on a honeycomb lattice. *Nature*

554, 341-345 (2018).

[7] K. W. Plumb, J. P. Clancy, L. J. Sandilands, V. V. Shankar, α-$RuCl_3$: A spin-orbit assisted Mott insulator on a honeycomb lattice. *Phys. Rev. B* **90**, 041112(R) (2014).

[8] J. A. Sears, *et al.*, Magnetic order in α-$RuCl_3$: A honeycomb-lattice quantum magnet with strong spin-orbit coupling. *Phys. Rev. B* **91**, 144420 (2015).

[9] S.-H. Do, *et al.*, Majorana fermions in the Kitaev quantum spin system α-$RuCl_3$. *Nat. Phys.* **13**, 1079-1084 (2017).

[10] T. Suzuki, S.-I. Suga, Effective model with strong Kitaev interactions for α-$RuCl_3$. *Phys. Rev. B* **97**, 134424 (2018).

[11] I. Rousochatzakis, S. Kourtis, J. Knolle, R. Moessner, N. B. Perkins, Quantum spin liquid at finite temperature: Proximate dynamics and persistent typicality. *Phys. Rev. B* **100**, 045117 (2019).

[12] A. Glamazda, P. Lemmens, S.-H. Do, Y. S. Kwon, K.-Y. Choi, Relation between Kitaev magnetism and structure in α-$RuCl_3$. *Phys. Rev. B* **95**, 174429 (2017).

[13] Y. Kasahara, *et al.*, Majorana quantization and half-integer thermal quantum Hall effect in a Kitaev spin liquid. *Nature* **559**, 227-231 (2018).

[14] J. A. Sears, Y. Zhao, Z. Xu, J. W. Lynn, Y.-J. Kim, Phase diagram of α-$RuCl_3$ in an in-plane magnetic field. *Phys. Rev. B* **95**, 180411(R) (2017).

[15] A. U. B. Wolter, *et al.*, Field-induced quantum criticality in the Kitaev system α-$RuCl_3$. *Phys. Rev. B* **96**, 041405(R) (2017).

[16] S.-H. Baek, *et al.*, Evidence for a Field-Induced Quantum Spin Liquid in α-$RuCl_3$. *Phys. Rev. Lett.* **119**, 037201 (2017).

[17] A. Kitaev, Anyons in an exactly solved model and beyond. *Annals of Physics* **321**, 2-111 (2006).

[18] H. Théveniaut, M. Vojta, Bound states of fractionalized excitations in a modulated Kitaev spin liquid. *Phys. Rev. B* **96**, 054401 (2017).

[19] A. Stern, Non-Abelian states of matter. *Nature* **464**, 187-193 (2010).

[20] S. M. Winter, K. Riedl, D. Kaib, R. Coldea, R. Valenti, Probing α-$RuCl_3$ Beyond Magnetic Order: Effects of Temperature and Magnetic Field. Phys. Rev. Lett. **120**, 077203 (2018).

[21] A. Banerjee, *et al.*, Excitations in the field-induced quantum spin liquid state of α-$RuCl_3$. *npj Quantum Materials* **3**, 8 (2018).

[22] Z. Wang, *et al.*, Magnetic Excitations and Continuum of a Possibly Field-Induced Quantum

Spin Liquid in α-$RuCl_3$. *Phys. Rev. Lett.* **119**, 227202 (2017).

[23] A. N. Ponomaryov, *et al.*, Unconventional spin dynamics in the honeycomb-lattice material α-$RuCl_3$: High field electron spin resonance studies. *Phys. Rev. B* **96**, 241107(R) (2017).

[24] D. Takikawa, S. Fujimoto, Impact of off-diagonal exchange interactions on the Kitaev spin liquid state of α-$RuCl_3$. Preprint at https://arxiv.org/abs/1902.06433 (2019).

[25] L. J. Sandilands, Y. Tian, K. W. Plumb, Y.-J. Kim, K. S. Burch, Scattering Continuum and Possible Fractionalized Excitations in α-$RuCl_3$. *Phys. Rev. Lett.* **114**, 147201 (2015).

[26] A. Glamazda, P. Lemmens, S.-H. Do, Y. S. Choi, K.-Y. Choi, Raman spectroscopic signature of fractionalized excitations in the harmonic-honeycomb iridates β- and γ-Li_2IrO_3. *Nat. Commun.* **7**, 12286 (2016).

[27] J. Nasu, J. Knolle, D. L. Kovrizhin, Y. Motome, R. Moessner, Fermionic response from fractionalization in an insulating two-dimensional magnet. *Nat. Phys.* **12**, 912-915 (2016).

[28] J. Yoshitake, J. Nasu, Y. Kato, Y. Motome, Majorana-Magnon Crossover by a Magnetic Field in the Kitaev Model: Continuous-Time Quantum Monte Carlo Study. Preprint at https://arxiv.org/abs/1907.07299 (2019).

[29] K.-Y. Choi, *et al.*, Evidence for Dimer Crystal Melting in the Frustrated Spin-Ladder System $BiCu_2PO_6$. *Phys. Rev. Lett.* **110**, 117204 (2013).

[30] J. Knolle, D. L. Kovrizhin, J. T. Chalker, R. Moessner, Dynamics of fractionalization in quantum spin liquids. *Phys. Rev. B* **92**, 115127 (2015).

[31] J. Knolle, G.-W. Chern, D. L. Kovrizhin, R. Moessner, N. B. Perkins, Raman Scattering Signatures of Kitaev Spin Liquids in A_2IrO_3 Iridates with A = Na or Li. *Phys. Rev. Lett.* **113**, 187201 (2014).

[32] J. S. Gordon, A. Catuneanu, E. S. Sørensen, H.-Y. Kee, Theory of the field-revealed Kitaev spin liquid. *Nat. Commun.* **10**, 2470 (2019).